


The RSC complex remodels nucleosomes in transcribed coding sequences and promotes transcription in *Saccharomyces cerevisiae*

Emily Biemat, Jeena Kinney, Kyle Dunlap, Christian Rizza, and Chhabi K. Govind  *

Department of Biological Sciences, Oakland University, Rochester, MI 48309, USA

*Corresponding author: Mathematics and Science Building, Room 333, Department of Biological Sciences, Oakland University, 118 Library Dr., Rochester, MI 48309, USA. govind@oakland.edu

Abstract

RSC (Remodels the Structure of Chromatin) is a conserved ATP-dependent chromatin remodeling complex that regulates many biological processes, including transcription by RNA polymerase II (Pol II). We report that RSC contributes in generating accessible nucleosomes in transcribed coding sequences (CDSs). RSC MNase ChIP-seq data revealed that RSC-bound nucleosome fragments were very heterogeneous (~80 bp to 180 bp) compared to a sharper profile displayed by the MNase inputs (140 bp to 160 bp), supporting the idea that RSC promotes accessibility of nucleosomal DNA. Notably, RSC binding to +1 nucleosomes and CDSs, but not with -1 nucleosomes, strongly correlated with Pol II occupancies, suggesting that RSC enrichment in CDSs is linked to transcription. We also observed that Pol II associates with nucleosomes throughout transcribed CDSs, and similar to RSC, Pol II-protected fragments were highly heterogeneous, consistent with the idea that Pol II interacts with remodeled nucleosomes in CDSs. This idea is supported by the observation that the genes harboring high-levels of Pol II in their CDSs were the most strongly affected by ablating RSC function. Additionally, rapid nuclear depletion of Sth1 decreases nucleosome accessibility and results in accumulation of Pol II in highly transcribed CDSs. This is consistent with a slower clearance of elongating Pol II in cells with reduced RSC function, and is distinct from the effect of RSC depletion on PIC assembly. Altogether, our data provide evidence in support of the role of RSC in promoting Pol II elongation, in addition to its role in regulating transcription initiation.

Keywords: transcription initiation

Introduction

The nucleosome is the fundamental unit of chromatin and is formed by wrapping ~147 base pairs of DNA around an octamer of histones (2 copies of H3, H4, H2A, and H2B). DNA wrapped around a histone octamer is largely inaccessible for DNA-dependent processes, including transcription by RNA polymerase II (Pol II) (Lorch *et al.* 1987). This nucleosomal impediment can be relieved by chromatin remodeling complexes that use the energy derived from ATP hydrolysis to slide or evict histones in order to expose the underlying DNA (Clapier and Cairns 2009; Clapier *et al.* 2016). One such remodeler is the SWI/SNF family member RSC (Remodels the Structure of Chromatin) complex, the only essential remodeler in budding yeast (Cairns *et al.* 1996).

RSC is an important regulator of chromatin organization around gene promoters. It is implicated in establishing 'nucleosome depleted regions' (NDRs) found upstream of transcription start sites (TSSs) and in positioning of the NDR-flanking nucleosomes referred to as the -1 and +1 nucleosomes (-1_Nuc and +1_Nuc) (Krietenstein *et al.* 2016). The DNA sequence forming the +1_Nuc often harbors the TSS, and the +1_Nuc can therefore be

inhibitory to transcription initiation. RSC has been reported to bind to both the -1_Nuc and +1_Nuc, and impairing RSC function is associated with the movement of flanking nucleosomes toward the NDR, which results in filling of the NDRs (Badis *et al.* 2008; Hartley and Madhani 2009; Ganguli *et al.* 2014; Kubik *et al.* 2015; Rawal *et al.* 2018; Brahma and Henikoff 2019; Klein-Brill *et al.* 2019). Nucleosomes that invade or assemble within NDRs are also cleared by RSC (Kubik *et al.* 2015; Brahma and Henikoff 2019). These nucleosomes were bound by RSC and were termed "fragile", given their greater sensitivity to digestion by micrococcal nuclease (MNase). The presence of such nucleosomes is controversial, partly due to the difficulty in detecting them by conventional ChIP-seq methods (Chereji *et al.* 2017). Although recent studies provide evidence for the presence of fragile nucleosomes (Brahma and Henikoff 2019), the role of such nucleosomes in transcription, however, is not yet clear. In addition to RSC, general regulatory factors (GRFs) and underlying DNA sequences play a role in NDR formation and maintenance (Krietenstein *et al.* 2016; Kubik *et al.* 2018).

The role of RSC in regulating chromatin structure at promoters is also linked to transcription. When cells were depleted

Received: December 23, 2020. **Accepted:** February 05, 2021

© The Author(s) 2021. Published by Oxford University Press on behalf of Genetics Society of America.

This is an Open Access article distributed under the terms of the Creative Commons Attribution-NonCommercial-NoDerivs licence (<http://creativecommons.org/licenses/by-nc-nd/4.0/>), which permits non-commercial reproduction and distribution of the work, in any medium, provided the original work is not altered or transformed in any way, and that the work is properly cited. For commercial re-use, please contact journals.permissions@oup.com

of the catalytic RSC subunit Sth1, the resulting shift in nucleosomes towards NDRs was associated with reduced Pol II and TBP occupancies at many genes (Kubik et al.2018; Rawal et al.2018), as well as with reduced TSS utilization and transcription (Klein-Brill et al.2019; Kubik et al.2019). RSC is also suggested to play a post-initiation role in promoting transcription. For example, RSC promotes Pol II elongation through acetylated nucleosomes in vitro (Carey et al.2006) and localizes to transcribed coding sequences (CDSs) in vivo (Ganguli et al.2014; Spain et al.2014). Cells deficient for both RSC (Sth1) and SWI/SNF (Snf2) displayed reduced Pol II occupancy at targets of Gcn4 under conditions of amino acid starvation (Rawal et al.2018). Notably, the CDSs of Gcn4 targets were also enriched for RSC (Spain et al.2014) and SWI/SNF (Rawal et al.2018). Moreover, depleting Rsc8 (RSC subunit) altered distribution of Pol II along coding regions (Ocampo et al.2019). These results suggest that the role of RSC in promoting transcription might extend to post-initiation steps, and could include remodeling nucleosomes immediately downstream of elongating Pol II in CDSs.

To address a potential role for RSC in promoting transcription by increasing DNA accessibility in CDSs, we performed ChIP-seq using MNase-digested chromatin and mapped RSC at a nucleosomal resolution. We then analyzed the length of DNA associated with RSC-bound nucleosomes (RSC_Nucs). We found that RSC was enriched in CDSs of highly transcribed genes, as reported previously (Spain et al.2014). RSC_Nucs were very sensitive to MNase digestion, displaying a more heterogenous fragment size distribution (~80 to 180 bp) compared to input nucleosomes, which showed a relatively sharper profile (~140 to 160 bp). This suggests that not only does RSC bind to nucleosomes in CDSs but also remodels them such that they are more susceptible to MNase digestion relative to the canonical nucleosomes. Such nucleosomes might therefore be more accessible to transcribing polymerases. In support of this idea, we found that Pol II-bound nucleosomes (Rpb3_Nucs) were very sensitive to MNase-digestion. Moreover, rapid nuclear-depletion of Sth1 led to accumulation of Pol II in CDSs of highly transcribed genes despite significant reductions in TBP binding, suggesting a slower clearance of Pol II from CDSs in absence of RSC function. Altogether, our data provide support for a model where RSC promotes transcription initiation by regulating nucleosome positioning and occupancy near the TSSs, and Pol II elongation by remodeling nucleosomes in transcribed regions.

Materials and methods

Yeast strain construction and growth conditions

The *Saccharomyces cerevisiae* strains used in this study are listed in Supplementary Table S1. Myc-tagged strains were generated as described previously (Govind et al.2012). Briefly, the plasmid pFA6a-13xMyc-His3MX6 was used as a template to PCR amplify the 13xMyc region using primers containing homologous sequences flanking the stop codon of *STH1*. The amplified DNA was used for transformation, and the colonies were selected on synthetic complete plates lacking histidine (SC/His⁻). The transformants were confirmed by PCR for integration and expression of the tagged protein by western blot. Cells were grown in YPD at 30°C to an absorbance A_{600} of 0.7-0.8 before being crosslinked as described previously (Govind et al.2012). Briefly, 11 ml of the cross-linking solution (50 mM HEPES-KOH [pH 7.5], 1 mM EDTA, 100 mM NaCl, 11% formaldehyde) was added to 100 ml culture. Cultures were crosslinked for 15 minutes at room temperature with intermittent shaking, and the cross-linking was quenched

by adding 15 ml of 2.5 M glycine. Cells were collected by centrifugation at 4000 rpm at 4°C for 5 mins and were washed twice with chilled 1X TBS. Cell pellets were stored at -80°C until further use.

MNase digestion

Crosslinked cell pellets were thawed on ice and resuspended in pre-chilled 500 μ l FA-lysis buffer (50 mM HEPES-KOH [pH 7.5], 1 mM EDTA, 140 mM NaCl, 1% Triton X-100, 0.1% sodium deoxycholate) containing protease inhibitors. Approximately 500 μ l of acid-washed glass beads were added to the resuspended cells, and cells were disrupted for 45 min in a cold room and the cell-extracts were collected by centrifugation. The beads were washed once with 500 μ l FA-lysis buffer and the supernatant was pooled with the cell-extracts. The cell-extracts were centrifuged for 10 min at 4°C to collect chromatin pellet, which was washed twice with FA-lysis buffer, and subsequently resuspended in 600 μ l of NPS buffer containing 1 mM β -mercaptoethanol (0.5 mM spermidine, 0.075% IGEPAL, 50 mM NaCl, 10 mM Tris-HCl [pH 7.5], 5 mM MgCl₂, 1 mM CaCl₂). Chromatin digestion was carried out at 30°C for 12 minutes with different concentrations of micrococcal nuclease (MNase, Worthington Biochemicals; cat# LS004798). The digestion was stopped by adding EDTA to final concentration of 10 mM, and incubating samples on ice for 10 min. To determine the extent of digestion, DNA was purified from 50 μ l aliquots of MNase-digested chromatin and resolved on 2% agarose gel. The chromatin samples showing approximately 80% DNA fragments corresponding to ~150 bp were used for ChIP and library preparation.

Chromatin immunoprecipitation

ChIPs were performed using a slightly modified protocol described previously (Govind et al.2012). 60 μ l of anti-mouse magnetic beads were washed with PBS/BSA (5 mg/ml BSA) and incubated with 3 μ l of anti-Myc (Roche) or Anti-Rpb3 antibodies (Neoclone) in 150 μ l of PBS/BSA for 3 hours. Post-incubation, the beads were washed twice with PBS/BSA and were incubated with 300 μ l of MNase-digested chromatin for 3.5 hours. 150 μ l MNase chromatin was set aside as inputs. The beads were subsequently washed with the following buffers: once with PBS/BSA, twice each with FA-lysis buffer, wash-buffer II (50 mM HEPES-KOH, 500 mM NaCl, 1 mM EDTA, 0.1% sodium deoxycholate, 1% Triton-X 100), and wash-buffer III (10 mM Tris-HCl [pH8.0], 250 mM LiCl, 1 mM EDTA, 0.5% sodium deoxycholate, 0.5% NP-40 substitute), and finally once with 1X TE. The immunoprecipitated complexes were eluted once at 65°C by elution buffer I (50 mM Tris-HCl, 10 mM EDTA, 1% SDS) for 15 minutes and then by elution buffer II (10 mM Tris-HCl, 1 mM EDTA, 0.67% SDS) for 10 minutes at 65°C. The eluents from each elution steps were pooled and incubated overnight in a 65°C water-bath for reverse crosslinking alongside the inputs. The following day, the samples were treated with 5 μ l of proteinase K (20 mg/ml, Ambion, cat# AM2548) for 2 hours before the DNA was extracted twice with chloroform: isoamyl alcohol (IAA) and ethanol precipitated overnight at -80°C. The DNA was resuspended in 50 μ l 1X TE/RNase (10 μ g/ml) and quantified using the Qubit.

Library preparation and sequencing

ChIP DNA (7-10 ng) and the corresponding MNase-input DNA (50 ng) were processed for library preparation using the NEBNext Ultra II Library prep kit for Illumina (cat # E7465S) to generate MNase-seq and ChIP-seq libraries. BIOO Scientific NEXTFLEX ChIP-Seq barcode oligos (cat# NOVA-514122) were used for ligation and the libraries were amplified according to the

manufacturer instructions. The inputs were amplified for 9 cycles, and ChIP samples for 12 cycles. The DNA libraries were gel purified and sequenced using the Illumina HiSeq-4K in paired-end mode (50 bp) at the University of Michigan Advanced Genomics Core Facility in Ann Arbor, MI, USA.

Data analysis

Sequences were trimmed to remove adapters using Cutadapt (parameter: -m 20) and were aligned to the *S. cerevisiae* genome (SacCer3) using Bowtie2 (parameters: -X 1000 -very-sensitive -no-mix -no-unal). Samtools was used to sort, index, and remove PCR duplicates from the bam files. After alignment, the number of paired-end reads for MNase inputs, Rpb3 ChIP-seq (MNase), RSC ChIP-seq (MNase), and Rpb3 ChIP-seq (sonicated chromatin) were ~ 46.8 million, 30.8 million, 23.7 million and 49.0 million, respectively. The data downloaded from the previous studies (Kubik et al.2018; Petrenko et al.2019) were similarly processed and analyzed as described below. The MNase-seq, MNase ChIP-seq and ChIP-seq bam files were analyzed using BamR (<https://github.com/rchereji/bamR>). The reads for each chromosome were set to 1 during normalization. The 2D-occupancy heatmaps were generated using the plot2DO.R. The fragments were aligned to their 5' end. Transcription start sites were taken from a previous study (Xu et al.2009). The single-end reads TBP and Pol II (Kubik et al.2018; Petrenko et al.2019) were normalized (10^6 reads) and analyzed using HOMER (v4.11, 10-24-2019). TBP occupancies were calculated from ± 200 bp of the TSS and Pol II occupancies were calculated from -100/+1000 bp of the TSS. Metagene profiles and scatterplots were generated in JMP (https://www.jmp.com/en_us/software/predictive-analytics-software.html). Boxplots were generated using the website <http://shiny.chemgrid.org/boxplotr/>. Venn diagrams were made using <http://www.biovenn.nl/>.

Data availability statement

Strains and plasmids are available upon request. Supplemental files are available at FigShare. Figure S1 shows nucleosome profiles generated by MNase-seq, Pol II ChIP-seq profiles and correlation between biological replicates for all datasets. The histograms depicting the MPDF profiles from the two earlier studies (Kubik et al.2018; Rawal et al.2018) are also shown. Figure S2 shows RSC enrichment in transcribed CDSs genome-wide. Figure S3 shows two-dimensional RSC MNase ChIP-seq profiles for replicates. Figure S4 shows genome-browser shots of Pol II and nucleosome occupancies in WT and Sth1 anchor-away cells (Kubik et al.2018). Table S1 provides names and genotype of the strains used in this study. The accession numbers for the raw and analyzed data reported in this paper are GSE147065. Supplemental Material available at figshare: <https://doi.org/10.25386/genetics.13638047>.

Results

Nucleosomes in transcribed coding sequences are sensitive to MNase digestion

DNA is relatively more resistant to MNase digestion when it is wrapped around the histone octamer or protected by non-histone proteins. As such, sequencing of the MNase-protected DNA fragment (MPDFs) is widely used to determine precise nucleosome occupancy and positioning (Koerber et al.2009; Ramachandran et al.2017). Considering that nucleosomes inhibit transcription by limiting access to DNA, we sought to determine the location of accessible nucleosomes, and whether the presence of such nucleosomes correlates with transcription. To this end, we digested formaldehyde cross-linked chromatin with

MNase and subjected the purified DNA to paired-end deep sequencing. The data MNase replicates were nearly identical to each other (Figure S1A; compare MNase inputs).

The majority of DNA fragment lengths from the MNase-digested chromatin was between 100 and 200 bp, with the peak centered around 150 bp (Figure S1B and S1C), consistent with the length of DNA protected by a canonical nucleosome (Henikoff et al.2011; Ramachandran and Henikoff 2016a; Ramachandran et al.2017). Heatmaps showing normalized MNase-seq read density for fragments for all yeast genes (5764 genes) displayed NDRs upstream of the TSS (Figure S1D). As expected, wider NDRs and lower nucleosome occupancies in both promoters and CDSs were observed at the most-highly transcribed genes (Figure S1D; compare the top of the heatmaps) when genes were sorted by descending order of their average Pol II ChIP-seq occupancies within their CDSs (Figure S1E). These results are consistent with the idea that histones are evicted both from promoters and from CDSs in the course of transcription, especially in highly-transcribed genes (Dion et al.2007).

The unwrapping of nucleosomal DNA or the ejection of H2A/H2B dimers by remodelers could make the nucleosomal DNA more susceptible to digestion by MNase, yielding MPDFs shorter than 147 bp, as shown previously (Ramachandran et al.2017; Brahma and Henikoff 2019) (Figure 1A). To determine the abundance of shorter fragments genome-wide in yeast, we analyzed MNase-seq data according to different MPDF lengths. A smaller enrichment for the shorter MPDFs relative to the canonical nucleosomes was evident for almost all nucleosomes (Figure 1B, compare black trace with other colored traces). However, the most enrichment for the shorter MPDFs (<120 bp) was evident at the -1 and -2 positions, similar to what was observed in *Drosophila* cells (Ramachandran et al.2015; Ramachandran and Henikoff 2016b). The shorter MPDFs at the -1 and -2 positions might reflect the chromatin remodeling that ensues during transcription in the promoter-proximal regions upstream of NDRs. Enrichment of H2AZ-containing nucleosomes at the -1 and +1 positions could also facilitate the generation of shorter MPDFs considering that H2AZ-containing nucleosomes are nucleosomes less stable (Weber et al.2014). Although some fraction of these fragments might also be generated by protection imparted by factors other than nucleosomes, for simplicity, we will refer to particles generating shorter MPDFs (<130 bp) as sub-nucleosomal particles.

We next asked whether the CDSs of highly-transcribed genes display greater abundance of shorter MPDFs considering that nucleosomes might be remodeled to promote Pol II elongation. To this end, we selected the top 10% (Pol II-T10) and the bottom 10% (Pol II-B10) of Pol II-occupied genes, and examined both gene-sets for MPDFs >130 bp and <130 bp (Figure 1C). We found that the Pol II-B10 genes displayed higher canonical nucleosome occupancies compared to Pol II-T10 genes (Figure 1C; compare dark red and dark blue traces), and also displayed enrichment of MPDFs >130 bp over MPDFs <130 bp (compare dark and light red traces) at the +2 to +6 positions. In contrast, Pol II-T10 genes showed a higher enrichment of the shorter fragments (<130 bp vs >130 bp; light and dark blue traces), both in CDSs as well as in promoters. A relatively greater digestion of nucleosomes by MNase in highly transcribed CDSs (Pol II-T10) might suggest that they are more accessible compared to those in the less-transcribed CDSs (Pol II-B10).

To determine whether shorter fragments are generated in a manner dependent on transcription, we examined the MPDFs for genes that are generally transcriptionally inactive and are greatly induced under amino acids starvation (Govind et al.2005; Rawal

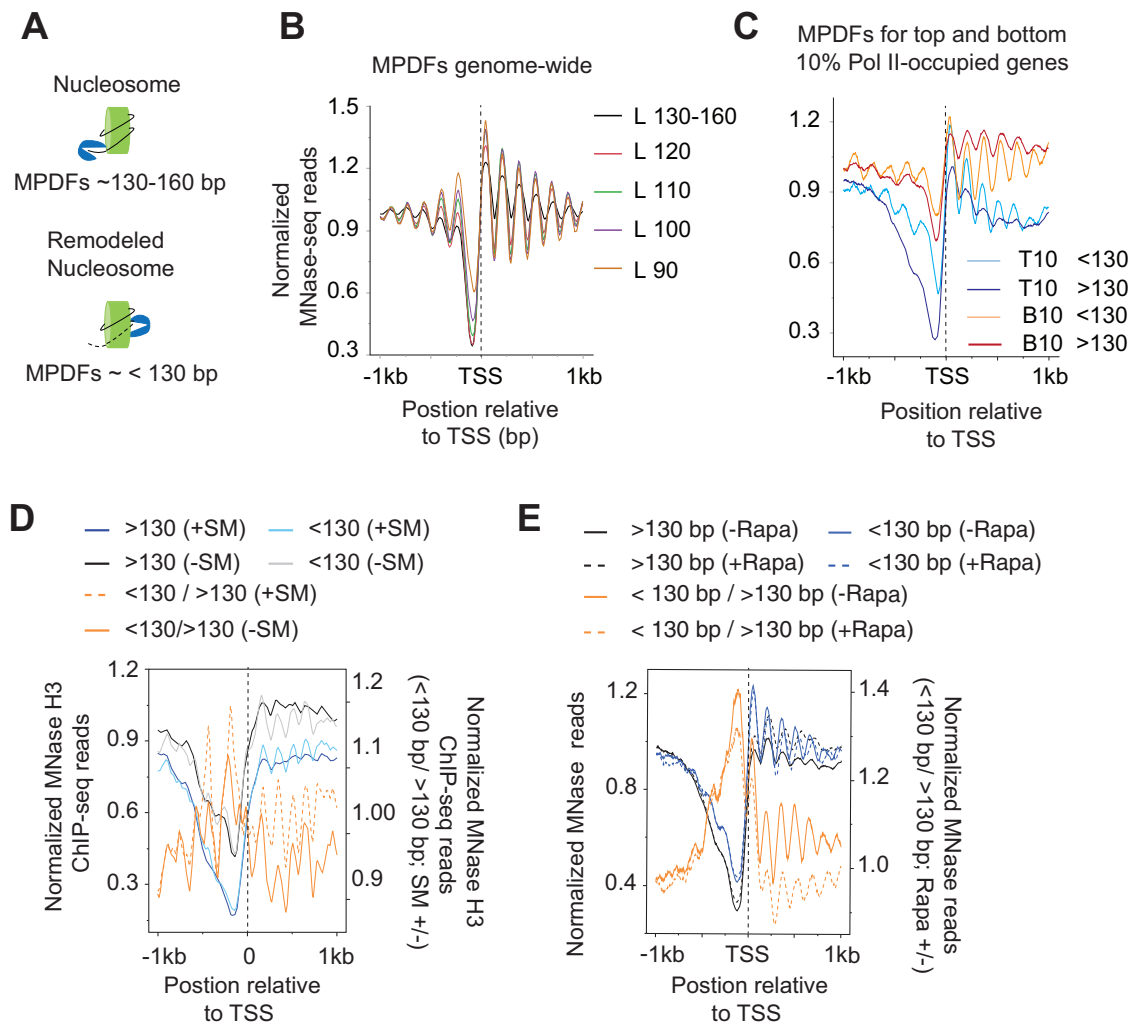


Figure 1 Nucleosomes in transcribed coding sequences are more susceptible to MNase digestion.

(A) Schematic showing potential generation of MNase-protected DNA fragments (MPDFs) from nucleosomes. MNase digestion of DNA wrapped around histone octamer would likely generate MPDFs ~130–160 bp, whereas a remodeled nucleosome might be more accessible, leading to shorter MPDFs (<130 bp).

(B) MPDF profiles for fragment lengths ranging from 130–160 bp, <120–110 bp, <110–100 bp, <100–90 bp, and <90 bp are plotted for 5746 genes. MPDFs are plotted ± 1000 bp around the transcription start site (TSS).

(C) Metagenes profile showing the average occupancies of MPDFs for the top (Pol II-T10) and bottom 10% (Pol II-B10) Pol II-occupied genes. MPDFs sizes <130 bp and >130 bp are plotted ± 1000 bp around the TSS.

(D) Metagenes profiles showing the average occupancies of MPDFs for the Gcn4-activated genes ($n = 70$ (Rawal et al. 2018)) induced in the presence of SM (sulfometuron methyl; +SM) or in the absence of SM (-SM). MPDFs sizes <130 bp and >130 bp are plotted ± 1 kb around the TSS. The values are plotted on the left-hand Y-axis, and <130 bp/>130bp ratios for +SM (dashed-orange traces) and -SM (orange traces) are plotted on the right-hand Y-axis.

(E) Metagenes profiles showing MPDFs sizes (<130 bp and >130 bp) for the TBP anchor-away strain treated without Rapa (-Rapa) or with (+Rapa) at the Pol II-T10 genes. The values are plotted on the left-hand Y-axis, and <130 bp/>130bp ratio for the -Rapa (orange trace) and +Rapa (orange dashed trace) are plotted on the right-hand Y-axis. The TBP anchor-away data was taken from a previous study (Kubik et al. 2018). MPDFs sizes <130 bp and >130 bp are plotted ± 1000 bp around the TSS.

et al. 2018). Treatment of cells with sulfometuron methyl (SM), an inhibitor of isoleucine/valine, mimics amino acid starvation and translationally induces expression of transcription activator Gcn4, which activates the transcription of the majority of the amino acid biosynthesis genes (Natarajan et al. 2001; Govind et al. 2005). Seventy genes were shown to be highly induced by SM in a Gcn4-dependent manner (Rawal et al. 2018). The MNase digestion profile for the untreated (-SM) and SM-treated (+SM) were nearly identical, although untreated cells revealed a slightly higher proportion of shorter fragments compared to induced +SM cells (Figure S1F). As shown in Figure 1D, non-induced (-SM) cells had a relatively higher fraction of nucleosomal MPDFs (>130 bp) compared to shorter fragments (<130 bp; compare black and gray traces). Upon induction by SM, the same set of 70

genes show a significantly greater fraction of shorter MPDFs compared to nucleosomal fraction (Figure 1D; +SM, compare light blue with dark blue traces). The ratios of shorter/nucleosomal MPDFs (<130 bp/>130 bp) fragments considerably increases upon transcription activation (+SM) of these genes (Figure 1D; compare solid and dashed orange traces) indicating that shorter MPDFs in CDSs are dependent on transcriptional activation. To provide further evidence for the transcription-dependency, we examined changes in MPDFs in TBP anchor-away (TBP-AA) cells (Kubik et al. 2018). Treating TBP-AA cells with rapamycin (Rapa) depletes TBP from the nucleus by exporting to cytoplasm (Haruki et al. 2008) and reduces transcription (Kubik et al. 2018). The WT cells (-Rapa) showed a higher proportion of shorter MPDFs observed compared to the nucleosomal-length fragments

(Figure 1E; compare solid blue traces with solid black traces). In contrast, the levels of both shorter and nucleosomal fragments were very similar in the Rapa-treated TBP-AA cells (compare dashed black and blue traces). As such, TBP anchor-away reduces $<130\text{ bp}/>130\text{ bp}$ ratios in Rapa-treated cells (Figure 1E; compare dashed orange with solid orange traces), suggesting that loss of TBP function leads to reduced nucleosomal accessibility (Kubik et al.2018). The MNase digestion profile for untreated and Rapa-treated cells was nearly undistinguishable (Figure S1G). Data showing the appearance of shorter MPDFs upon transcription activation, and their reduction upon inhibiting transcription by TBP anchor-away, suggest that their generation is linked to active transcription. Collectively, the data support the idea that nucleosomes in transcribed CDSs are remodeled to make them more accessible to MNase digestion or are converted to hexasomes, which have been shown to allow Pol II traversal through chromatin templates *in vitro* (Kireeva et al.2002; Kulaeva

et al.2007) and are shown to be present *in vivo* (Ramachandran et al.2017). Given that accessible nucleosomes are strongly dependent on active transcription, several factors including elongating polymerases and chromatin remodelers could help in generating accessible nucleosomes in transcribed regions.

RSC localizes to nucleosomes of highly transcribed genes

RSC plays important roles in maintaining NDRs near promoter regions (Musladin et al.2014; Kubik et al.2015; Krietenstein et al.2016; Kubik et al.2017), and has been implicated in promoting transcription (Carey et al.2006; Spain and Govind 2011; Ganguli et al.2014; Spain et al.2014; Rawal et al.2018; Ocampo et al.2019). The ability of RSC to slide nucleosomes to widen NDRs appears to enhance pre-initiation complex (PIC) assembly and TSS selection (Kubik et al.2018; Klein-Brill et al.2019; Kubik et al.2019). In addition, RSC is suggested to promote transcription by facilitating

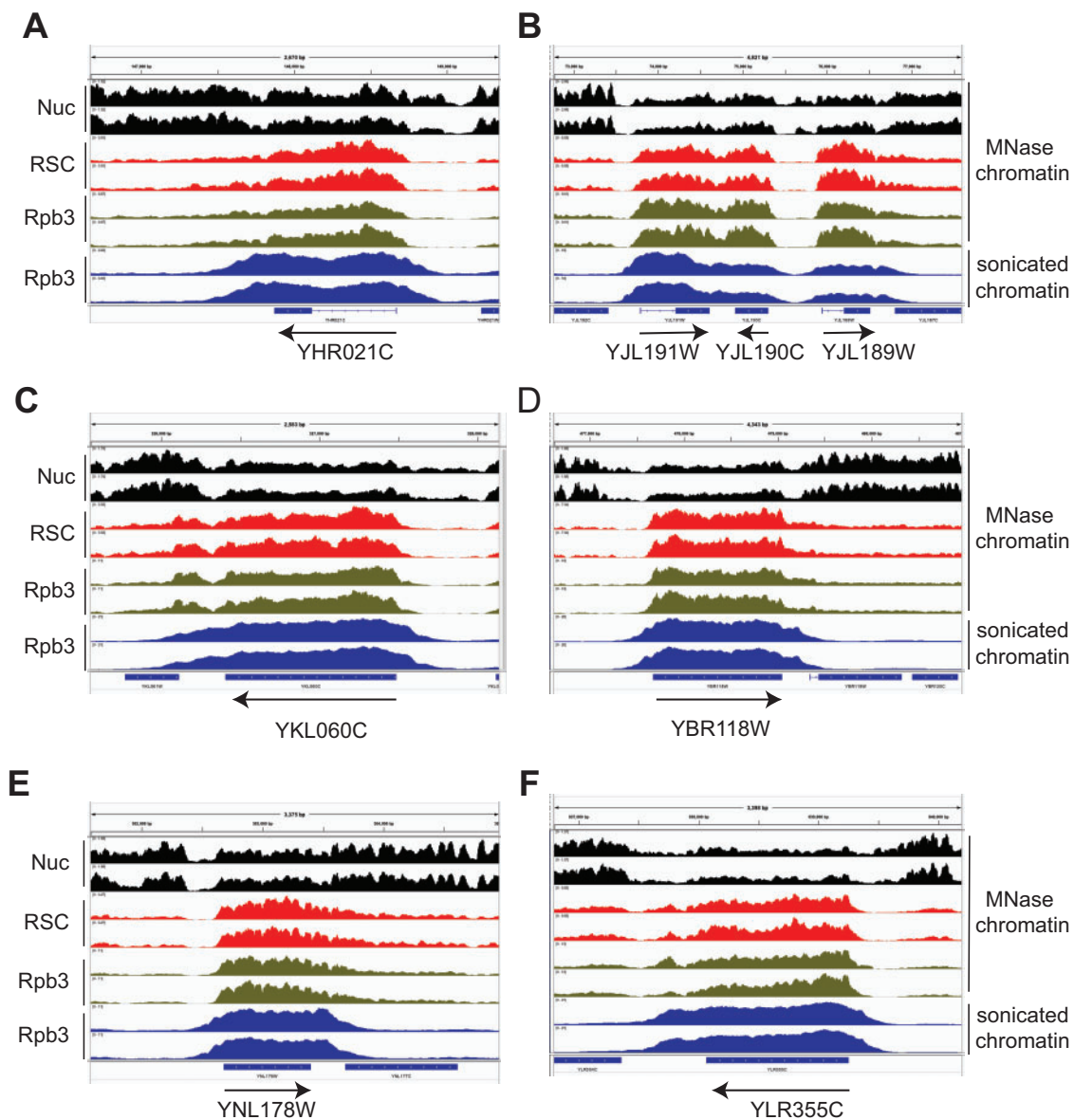


Figure 2 RSC localizes to nucleosomes of many highly transcribed genes.

(A-F) Genome-browser shots are shown for a few representative genes showing high RSC occupancies in their CDSs. Nucleosomes (Nuc; MNase inputs, black), RSC MNase ChIP-seq (red), Rpb3 MNase ChIP-seq (green) and sonicated chromatin Rpb3 ChIP-seq (blue) data are shown in panels (A-F). Arrows denote 5' to 3' direction. Biological replicates are shown.

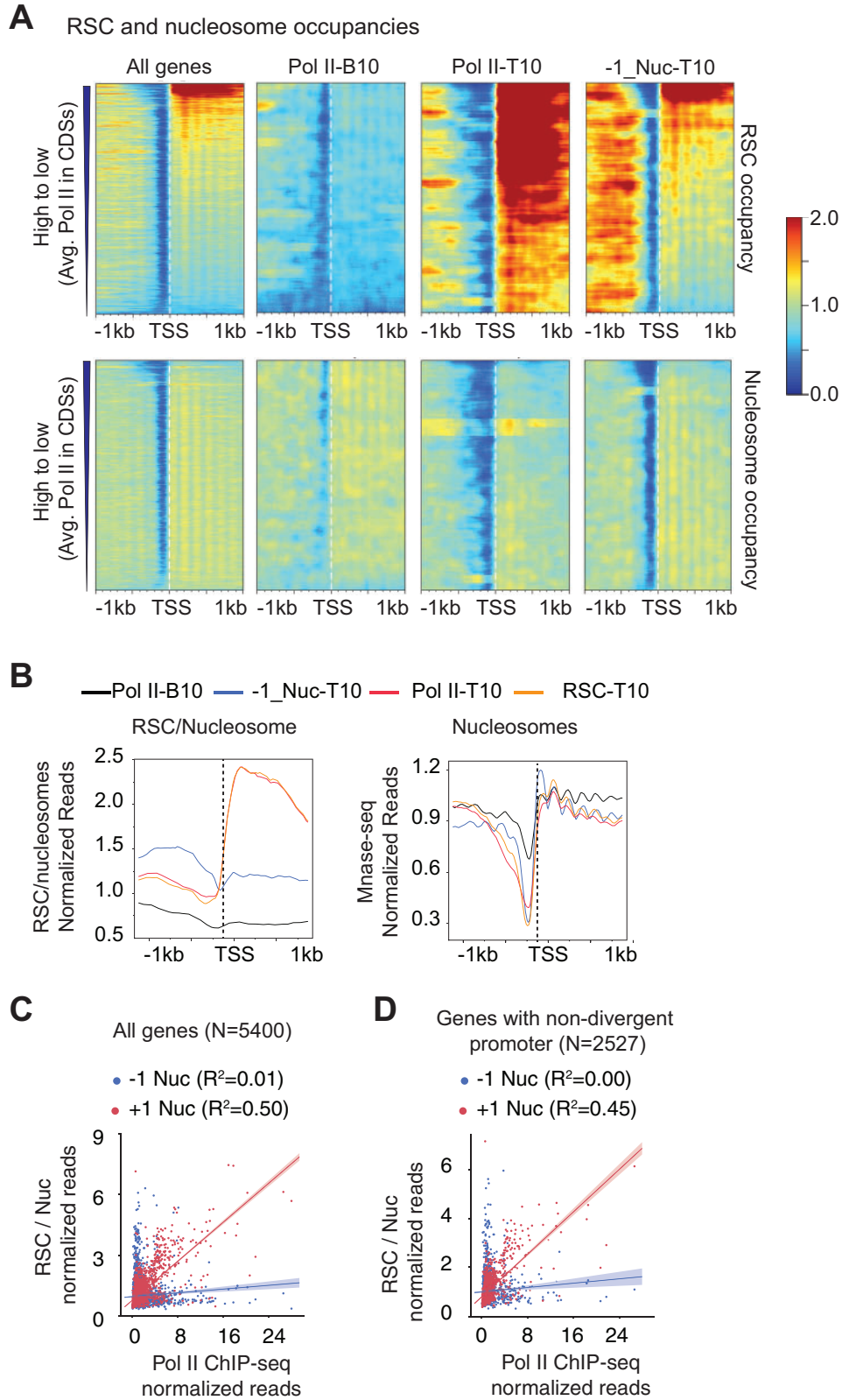


Figure 3 RSC enrichment in CDSs but not in promoters correlate with transcription.

(A) Heatmaps showing RSC (top panel) and nucleosome occupancies (bottom panel) are shown for all genes (~5700), Pol II-B10 ($n = 576$), Pol II-T10 genes ($n = 576$) and 576 genes with non-divergent promoters showing greatest RSC occupancy at the -1 nucleosome. The genes with divergent promoters were removed from all genes, and the top 576 genes showing greatest RSC occupancy at -1 position were selected (-1_Nuc-T10). RSC and nucleosome occupancies were sorted based on decreasing average Pol II occupancies in their CDSs.

(B) Metagene profiles for RSC/nucleosome ratios (top) and nucleosome occupancies (bottom) are shown for the indicated genes.

(C and D) Scatterplots showing correlations between RSC/nucleosome occupancies at -1 or +1 nucleosome positions, and average Pol II occupancies for all genes ($N = 5400$) (C), and for a subset of genes with non-divergent promoters ($N = 2527$) (D).

transcription elongation (Carey et al.2006; Spain and Govind 2011). In support of this possibility, we had previously provided genome-wide (ChIP-chip) evidence for localization of RSC in transcribed CDSs (Spain and Govind 2011; Spain et al.2014), which has subsequently been observed by other groups (Ganguli et al.2014; Vinayachandran et al.2018). Considering that RSC is enriched in CDSs of many transcribed genes, we sought to determine the role for RSC in enhancing nucleosome accessibility in CDSs. To this end, we ChIP-ed a myc-tagged form of Sth1, the catalytic subunit of the RSC complex, from MNase-digested chromatin and performed deep sequencing. In agreement with earlier studies (Spain and Govind 2011; Yen et al.2012), we observed a strong correlation between Pol II and RSC occupancies, genome-wide (Figure S1A). RSC was most enriched in the CDSs of highly transcribed genes, including those of ribosomal protein genes (RPGs) (Figures 2 and 3A, and Figures S1A and S2A). Consistent with this, Pol II-T10 genes substantially overlapped to those within the top 10% RSC-occupied genes (RSC-T10 genes henceforth; p -value = 4.8×10^{-333}). The metagene profiles for RSC occupancy normalized to nucleosomes clearly indicate the RSC is enriched primarily in the CDSs of the Pol II-T10 genes, and shows very little enrichment in their promoters (Figure 3B, left-hand panel; compare orange and red traces with black trace). The recruitment of RSC in CDSs is likely linked to transcription, considering our previous findings which showed that RSC was enriched in the CDSs of many amino acids biosynthetic genes (Gcn4 targets) only under Gcn4-inducing conditions in the WT cells but not in *gcn4Δ* cells or in non-induced cells (Spain et al.2014; Rawal et al.2018).

Several studies, including ours, have shown that RSC is enriched at promoters and upstream regulatory regions of many genes (Badis et al.2008; Yen et al.2012; Spain et al.2014; Kubik et al.2018; Brahma and Henikoff 2019). As RSC is implicated in sliding nucleosomes and in evicting histones during transcription (Rawal et al.2018), RSC binding to +1_Nuc might help in promoting transcription by promoting PIC assembly (Kubik et al.2018). Considering that MNase preferentially digests DNA in NDRs and the possibility that RSC-protected regions within the NDRs might have been lost during the MNase ChIP library preparation, we instead sought to identify those genes which harbored RSC at -1_Nuc and asked if such association is correlated with transcription. In this effort, we removed genes with divergent promoters, and we selected the top 576 genes from this subset of genes without divergent promoters. The top 576 genes (10% equivalent of all genes) with the highest RSC occupancies at -1 nucleosomes (-1_Nuc-T10) revealed that the RSC occupancies extended beyond -1_Nuc upstream of NDRs (Figure 3A; -1_Nuc-T10 panel). The genes with highest Pol II in this subset of genes (top of the heatmap) also displayed RSC occupancies in their CDSs, in addition to upstream regions. RSC occupancies at -1_Nuc weakly correlated with Pol II occupancies for all genes (Figure 3C; $p = 0.19$, $R^2 = 0.01$) and also for the subset of genes without divergent promoters (Figure 3D; $p = 0.22$, $R^2 = 0.00$). By contrast, a strong correlation was observed for RSC at +1_Nuc with Pol II occupancies (Figure 3C; $p = 0.58$, $R^2 = 0.50$) genome-wide and the smaller subset of genes without divergent promoters (Figure 3C; $p = 0.56$, $R^2 = 0.45$). Altogether, the data suggests that RSC recruitment to the +1_Nuc is tightly linked to Pol II occupancies (and transcription) at a genome-wide level.

RSC-bound nucleosomes are more susceptible to MNase digestion

Considering that nucleosomes in both promoters and CDSs displayed a presence of shorter MPDFs, we asked whether RSC

preferentially associates with intact nucleosomes (>130bp) or with partially-unraveled/subnucleosomal particles (<130bp). Although the MNase-inputs for lowly transcribed genes (Pol II-B10) displayed very similar levels of both nucleosomal and subnucleosomal particles (Figure 4A; compare gray black and gray traces), enrichment for the nucleosomal fraction was slightly higher for the RSC-bound nucleosomes (RSC_Nucs) (Figure 4A; compare red vs orange traces). Thus, there was a very little enrichment of fragments corresponding to subnucleosomal particles in RSC_Nucs for the Pol II-B10.

For the highly transcribed genes (Pol II-T10), the MNase inputs displayed a slightly higher proportion of sub-nucleosomal particles relative to nucleosomes (Figure 4B; compare black and grey traces). However, the overall levels were very similar to Pol II-B10 genes (compare Nucs in Figure 4A and 4B, and Figures S3A and S3B). By contrast, both nucleosomal and subnucleosomal particles were substantially enriched in the RSC_Nucs on Pol II-T10 genes compared to Pol II-B10 (Figure 4B). Notably, however, the RSC_Nucs were more enriched for the shorter fragments relative to the nucleosome-size fragments (Figure 4B, compare orange vs red traces). We also noted that the positioning of the RSC_Nucs appeared to be more diffuse, suggesting that RSC_Nucs could be more dynamically positioned compared to the canonical nucleosomes, especially those at highly transcribed genes.

The higher proportion of shorter MPDFs in RSC_Nucs raised a possibility that elevated RSC occupancy and attendant remodeling makes nucleosomes more susceptible to MNase digestion. To get a better idea of the distribution of DNA fragment sizes associated with RSC_Nucs, we performed a two-dimensional (2D) analysis of fragment-length distributions (Chereji et al.2017) of RSC_Nucs at the Pol II-B10, Pol II-T10, and RPGs that showed high RSC occupancies in their CDSs (Figure S2A) and compared them to the fragment-length distributions for all nucleosomes (MNase inputs) for the same genes. Such comparison allowed us to differentiate the remodeling status of RSC_Nucs from other nucleosomes in same region. As expected, both the promoters and CDSs of the Pol II-T10 and RPGs displayed lower nucleosome densities compared to the corresponding regions of the Pol II-B10 genes (Figure 4C). Despite the differences in nucleosome densities (MPDFs ~150 bp), the 2D fragment size distributions profiles were very similar for nucleosomes at these three gene-sets (Figures 4C, and 4E; left panel). RSC bound nucleosomes at the Pol II-B10 genes displayed only a slightly greater heterogeneity in fragment lengths compared to nucleosomes in the same region (Figure S3C). In contrast, the Pol II-T10 displayed a substantially higher fraction of shorter fragments in RSC_Nucs versus total nucleosomes (Figure 4, C and D and Figure S3D) and compared to the RSC_Nucs at the Pol II-B10 genes (Figure 4, C-E, blue vs. green and black traces, and Figures S3C and S3D, compare orange and blue traces). More importantly, the distribution of shorter fragments coincided with the RSC occupancy, as the majority of heterogeneity for the fragments for the Pol II-T10 genes was localized in the CDSs, where the majority of RSC is found. The abundance of shorter fragments also largely corresponded to RSC occupancies (Figure 4E). As such, the highest levels of shorter fragments were observed for the RPGs, followed by the Pol II-T10 genes (Figure 4, C-E). It is notable that the size distributions for the RSC_Nucs were very broad and relatively smooth as opposed to the discrete-sized fragments observed upon MNase over-digestion (Chereji et al.2018). Such profile fits with the remodeling activity of RSC, which gradually exposes DNA through its translocase activity (Clapier et al.2016). The upper limit of MPDFs (~180 bp) in RSC_Nucs could be due to the protection provided

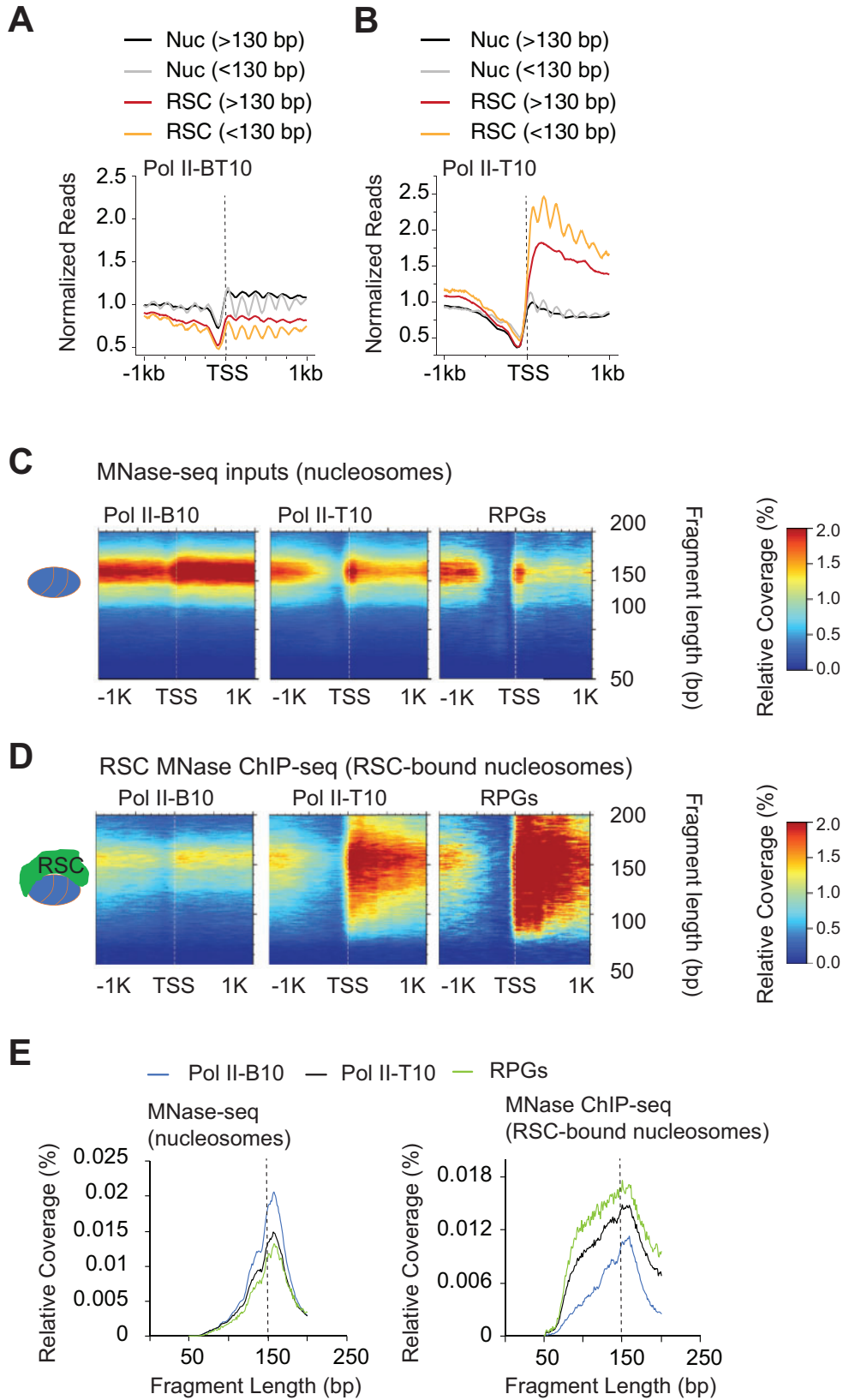


Figure 4 RSC associates with both full-length and shorter MPDFs.

(A and B): Metagene profile showing normalized reads of MPDFs corresponding to the nucleosomes (MNase inputs; Nuc) and RSC-bound nucleosomes (RSC MNase ChIP-seq; RSC) for the bottom 10% (A) and top 10% Pol II-occupied genes (B).

(C and D): Heatmaps depicting 2D-occupancies of MPDF distribution around the TSS, with MPDFs shown on the Y-axis. MPDFs from nucleosomes (C) and RSC-bound nucleosomes (D) at the bottom 10% Pol II-occupied genes, top 10% Pol II-occupied genes, and at RPGs. (E) Metagene profiles depicting the relative amount of fragment lengths for the nucleosomes (left panel) and RSC-bound nucleosome MPDFs (right panel) observed in (C) and (D).

due to formation of the RSC-nucleosome complex (Shukla *et al.*2010), whereas shorter MPDFs might represent partially unwrapped nucleosomes or hexasomes (Brahma and Henikoff 2019).

Although the fragment-size profiles for total nucleosomes in both infrequently transcribed (Pol II-B10) and highly transcribing genes are very similar (Figure 4E, left panel), the differences in RSC-Nucs profile (Figure 4E, right panel) suggests that unwrapped nucleosomes/hexasomes might only represent a small fraction of total nucleosomes in CDSs even at the very highly transcribing genes. Altogether, heterogenous fragment sizes for the RSC_Nucs is consistent with the idea that RSC binding to nucleosomes may help in exposing DNA to transcribing polymerase in CDSs, and potentially enhances transcription elongation. However, given that RSC occupies CDSs of highly transcribed genes, it is possible that partial unwrapping of nucleosomes by elongating polymerases might also facilitate RSC recruitment to further aid in remodeling of nucleosomes.

RNA polymerase interacts with MNase-sensitive nucleosomes In Vivo

Earlier studies have shown that Pol II tends to localize close to nucleosomes in coding regions (Churchman and Weissman 2011), and has been shown to interact with nucleosomes by MNase ChIP-seq (Koerber *et al.*2009). Considering that DNA from RSC_Nucs displayed very heterogenous fragment sizes and that the presence of RSC enhanced transcription *in vitro* through acetylated chromatin templates (Carey *et al.*2006), we sought to determine the accessibility status of Pol II-bound nucleosomes. We, therefore, performed Rpb3 (Pol II) ChIP-seq using the MNase digested chromatin used for examining RSC occupancies. To ensure that the nucleosomal-length fragments were ChIP-ed with Pol II, we examined Rpb3 ChIP-seq signals for MPDF lengths between 130–160 bp (Figure 5A). The 130-160 MPDFs are unlikely to be generated through protection imparted by elongating Pol II itself. The Pol II MNase ChIP-seq occupancy profile highly correlated with the Pol II occupancies determined by Rpb3 ChIP-seq

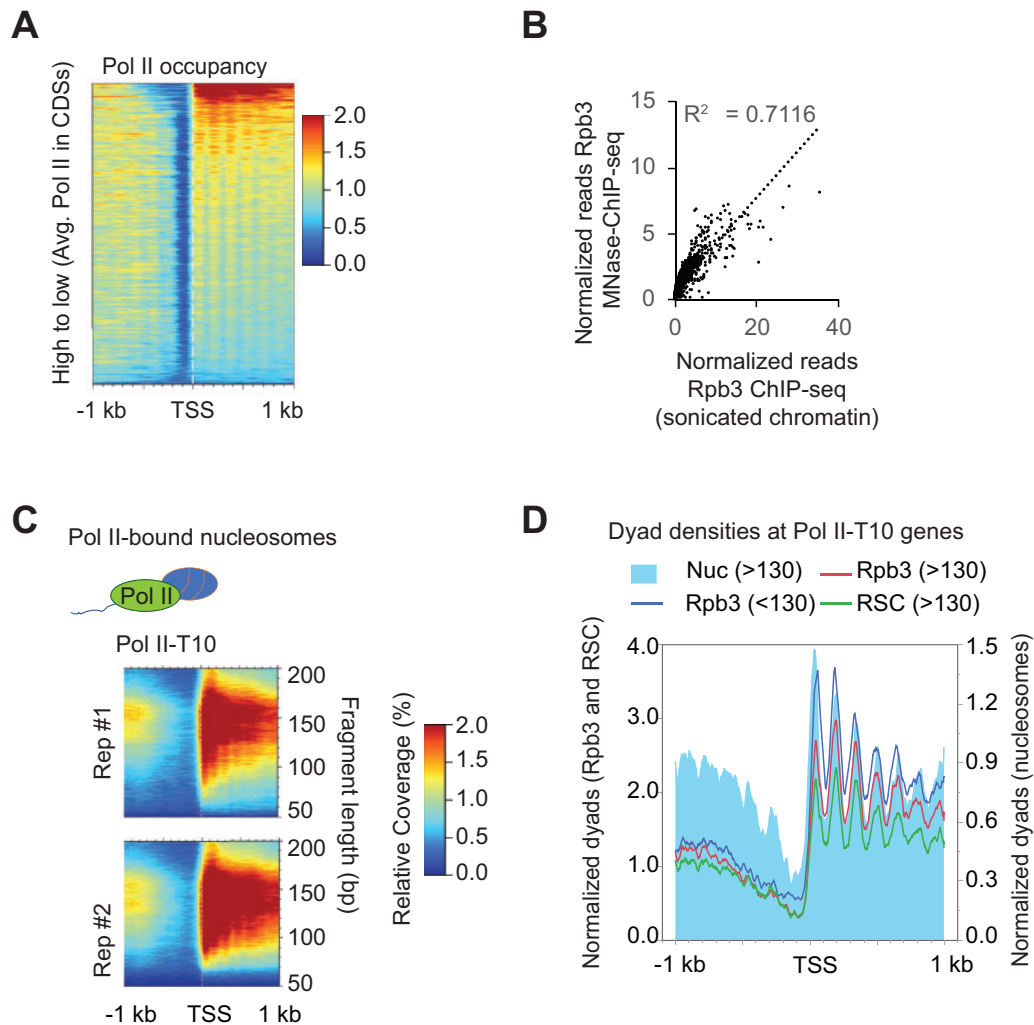


Figure 5 Pol II interacts with nucleosomes genome-wide.

(A) Heatmap showing Pol II occupancies from Pol-II MNase ChIP-seq data sorted by decreasing Pol II occupancies, which were determined by ChIP-seq using sonicated chromatin.

(B) Scatterplot depicting correlation between Rpb3 ChIP-seq occupancies from MNase and sonicated chromatin.

(C) 2D occupancy plots showing MPDF distribution obtained from Rpb3-bound nucleosomes for the top 10% of Pol II-occupied genes.

(D) Plot showing dyad densities for the Rpb3 (MPDFs: <130, blue trace; >130–160; red trace), MPDFs >130 for RSC (green) and nucleosomes (MNase inputs; filled blue).

analysis of sonicated chromatin (Figure 5B, $r=0.84$), suggesting that Pol II indeed interacts with nucleosomes (considering the strong Rpb3 signal for 130–160 MPDFs) and not merely naked DNA within the transcribed CDSs, genome-wide, in agreement with several previous studies (Kireeva et al.2002; Bondarenko et al.2006; Ujvari et al.2008; Kulaeva et al.2013).

We next examined the fragment size distribution for the Rpb3-bound nucleosomes (Rpb3_Nucs henceforth). The Rpb3_Nucs MPDF size distribution profile for the Pol II-T10 genes (Figure 5C) was very similar to that observed for the RSC_Nucs (Figure 4D). The frequent association of Pol II with subnucleosomal fragment lengths (<130bp, Figure 5C) suggests that MNase ChIP-seq captures the Pol II molecules that might be interacting with or traversing through nucleosomes, consistent with the recent cryo-EM structures of Pol II transcribing through nucleosomes (Farnung et al.2018; Kujirai et al.2018). The dyad positioning for the 130–160bp MPDFs (>130bp) of the MNase inputs were largely overlapping with those obtained from Rpb3 and RSC ChIP-seq (Figure 5D). The shorter MPDFs also largely overlapped with dyads of MNase inputs and were not exclusively present in the inter-nucleosomal regions. The similarity between the size distribution of the Rpb3_Nucs with RSC_Nucs (Figures 4C and 6C), and a strong correlation between RSC and Pol II occupancies (Figure 3C) suggests that RSC might help in Pol II elongation by increasing accessibility of nucleosomal DNA. If so, one might expect to see transcription defects upon ablating RSC function, especially at those genes which show high RSC occupancies in their CDSs.

RSC depletion differentially affects TBP and Pol II occupancies at highly transcribed genes

To assess the role of RSC in potentially regulating Pol II elongation, we analyzed data from the study (Kubik et al.2018), which used the anchor-away strategy (Haruki et al.2008) to rapidly deplete Sth1 from the nucleus, and examined the changes in nucleosome, TBP and Pol II occupancies, genome wide. The study showed that Pol II and TBP occupancies were significantly reduced in rapamycin (Rapa) treated Sth1 anchor-away (*sth1-aa*) cells and that these changes were correlated with the increased occupancies in nucleosomes in the promoter regions, genome-wide. We were interested in identifying those genes where RSC function might be attributed to promoting Pol II elongation in a manner that is distinguishable from its role in transcription initiation. Towards this goal, we first examined Pol II and TBP occupancies changes in deciles based on the WT Pol II occupancies using data from the Shore lab (Kubik et al.2018). As expected, TBP occupancies were reduced in all deciles except for the very last decile representing the set of genes with the lowest Pol II occupancies (Figure 6A). These results suggest that TBP binding is strongly dependent on RSC function. Intriguingly, however, Pol II occupancies did not decrease in the CDSs of genes that show high Pol II occupancies in WT cells (the first two deciles) despite reductions in average TBP binding at these genes. However, the 3rd to 9th deciles showed expected reductions in both TBP and Pol II occupancies. This is consistent with a recent study that showed a strong relationship between PIC assembly and Pol II occupancies, genome-wide (Petrenko et al.2019). The genes in the top two deciles, which showed unexpectedly higher Pol II occupancies in *sth1-aa* cells, showed expected reductions in Pol II in TBP anchor-away cells (Figure 6B; data from Petrenko et al.2019). The meta-gene plots revealed that Pol II occupancies were higher in the *sth1-aa* (Rapa) cells across the CDS compared to untreated (no Rapa) cells despite reductions in TBP levels in promoters of Pol II-

T10 genes (Figure 6C, left-hand panel). In contrast, both TBP and Pol II occupancies were reduced at the genes which showed the greatest defect in TBP binding upon Sth1 anchor-away (Figure 6C, right-hand panel). Thus, it appears that genes which harbor high-levels of Pol II and RSC in their CDSs respond differently to rapid depletion of RSC than the rest of the genes, in that they are less responsive to the reductions in TBP binding at their promoters (presumed initiation defects).

It is possible that a subset of genes within the first two deciles contributes to the intriguing disconnect between TBP occupancy and Pol II in CDSs in response to Sth1 depletion. It was shown earlier that RPGs, which are amongst the highly transcribed genes, were largely unaffected by rapid depletion of Sth1 in that they show minimal changes in nucleosome occupancy (Kubik et al.2018). Therefore, presence of RPGs in the top deciles might account for the aberrant Pol II behavior upon Sth1 depletion. In this regard, we examined the genes within the first decile that show higher Pol II on Sth1 depletion (Figure 6D). Within the first decile, both Pol II and TBP occupancies were reduced at 34% genes (191 out of 570). In contrast, a greater proportion of genes (~66%), including 107 RPGs, showed increased Pol II occupancy and reduced TBP binding upon Sth1 anchor-away. Increased Pol II occupancy was evident even after removing RPGs from this subset of genes. Thus, 296 highly Pol II-occupied genes showed similar effects on Pol II occupancies as the ribosomal protein genes after the loss of RSC function. The second decile also contained a subset of genes that showed higher Pol II in CDSs in response to Sth1 anchor-away (Figure 6E; 227 genes out of 570 genes).

RSC aids in generating accessible nucleosomes

Increased Pol II occupancies upon Sth1 anchor-away, particularly in highly expressed genes (based on Pol II occupancies), is consistent with a decreased rate of Pol II elongation in a manner that obscures the effects of RSC loss on PIC assembly (TBP occupancy). Given that Pol II-T10 genes are highly enriched for RSC in their CDSs, it is possible that nucleosome accessibility to polymerases is reduced in *sth1-aa* cells such that it increases dwell-time for the elongating Pol II, leading to an increased crosslinking of Pol II in CDSs. Towards this, we analyzed MNase-seq data (Klein-Brill et al.2019) in which Sth1 was depleted using auxin-induced degradation (AID) (Nishimura et al.2009) to determine the contribution of RSC in nucleosome accessibility. We focused on the subset of genes that did not show reduction in Pol II occupancy upon Sth1 anchor-away (Figure 6D). As Pol II itself can render nucleosomes accessible, it is possible that higher Pol II in RSC-deficient cells might increase the proportion of shorter/nucleosomal (<130/>130bp) MPDFs in CDSs. Alternately, if RSC contributes to the generation of accessible nucleosomes, then Sth1 depletion might reduce these ratios, despite increased Pol II occupancies in the CDSs. For RPGs, Sth1 depletion led to an increase in nucleosomal fragments in the CDSs (Figure 7A; compare yellow with blue traces) and a decrease in shorter/nucleosomal MPDF ratios (<130bp/>130bp) in both promoters and CDSs. Likewise, the ratios were also reduced for the 379 genes that did not show reduction in Pol II occupancy in *sth1-aa* cells (Figure 7B). In both cases, we noted that there was a significant reduction in the ratios at the promoter (Figure 7, A and B) and that this might reflect reduction in PIC formation in Sth1-depleted cells, consistent with reduced TBP binding (Figure 6D). Thus, the data show that the proportion of accessible nucleosomes is reduced in the CDSs of those genes which do not show reduced Pol II occupancy in cells impaired for RSC function, suggesting that RSC may affect

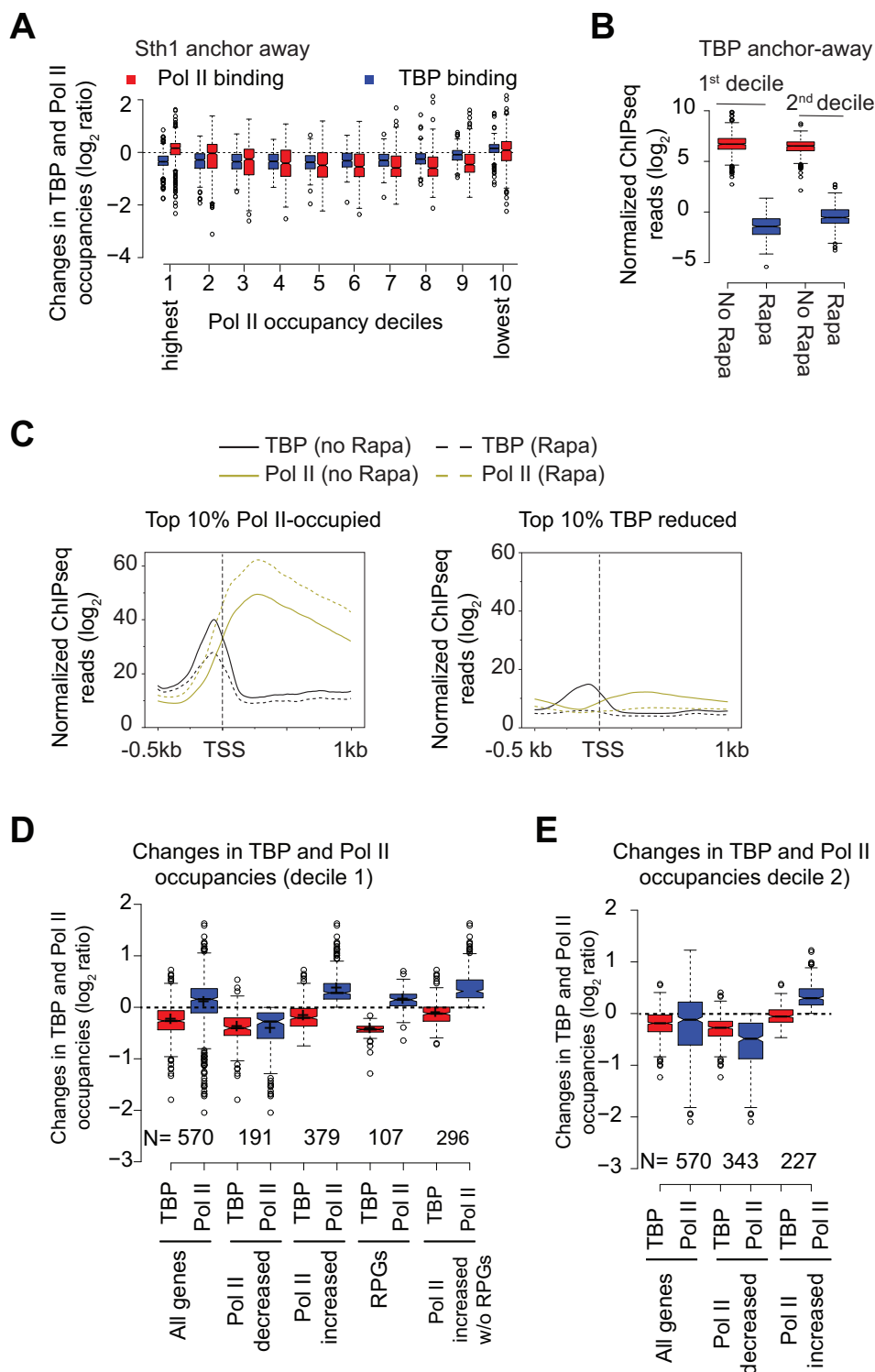


Figure 6 Nuclear depletion of RSC differentially affects TBP and Pol II occupancies at highly transcribed genes.

The data analyzed in this Figure was obtained from previous studies (Kubik et al.2018) and (Petrenko et al.2019).

(A) Boxplot showing changes in TBP and Pol II binding in Sth1 anchor-away cells (+ Rapa) in deciles based on WT Pol II occupancies (data from Kubik et al.2018). Decile 1 and decile 10 represents the most and the least Pol II-occupied genes, respectively.

(B) Boxplot showing Pol II occupancies for the top 2 deciles of Pol II-occupied genes in untreated and Rapa-treated TBP anchor-away cells.

(C) Metagenes plots showing TBP and Pol II occupancies for the top 10% Pol II-occupied genes (left-hand panel) and the top 10% genes showing the most reductions in TBP binding (right-hand panel) in untreated and Rapa-treated Sth1 anchor-away cells.

(D) Boxplots showing TBP and Pol II occupancy for the top decile of Pol II-occupied genes (All genes) and the genes that show reduction in Pol II occupancy (Pol II decreased) upon Sth1 anchor-away. Occupancies are also shown for the genes within the top decile that show increase in Pol II occupancy (Pol II increased) upon Sth1 anchor-away and also for the same gene-set after excluding RPGs. The occupancies for RPGs are also shown.

(E) Boxplots showing TBP and Pol II occupancy for the 2nd decile of Pol II-occupied genes (All genes), the genes that show reduction in Pol II occupancy (Pol II decreased) and those that do not show any decrease (Pol II increased) upon Sth1 anchor-away.)

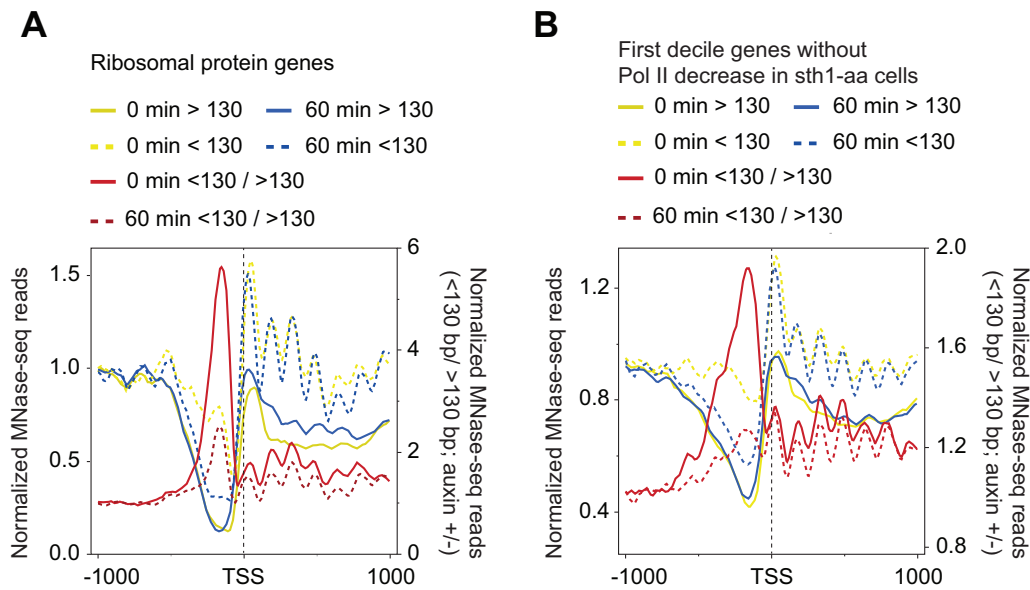


Figure 7 RSC contributes to nucleosome accessibility in CDSs.

(A and B) MDPF analysis for ribosomal proteins genes (A) and the genes in the top decile of the Pol II-occupied genes (B) at 0 minutes and at 60 minutes after treatment of *STH1-AID* strain with auxin to rapidly deplete Sth1. The MNase-seq data for this analysis was obtained from a previous study (Klein-Brill et al.2019).

the ability of elongating polymerases to navigate nucleosomes. Determining nascent RNA levels in Sth1-depleted cells might provide more direct evidence for the role of RSC in promoting transcription elongation.

Discussion

Our data suggest that RSC recruitment to coding sequences promotes transcription in part by making nucleosomes in CDSs more accessible to elongating polymerases. This is supported by the evidence that nucleosomes in highly transcribed CDSs are more accessible and that this accessibility is both RSC- and transcription-dependent. RSC-bound nucleosomes within CDSs are highly susceptible to MNase digestion, suggesting that remodeling by RSC might make DNA accessible to transcribing Pol II. Consistent with this idea, we find that the Pol II-bound nucleosomes were also digested to a greater extent than the canonical nucleosomes in the same regions of those genes which showed RSC occupancies in their CDSs (Figure 5).

Given that a single nucleosome is a potent barrier for Pol II elongation (Lorch et al.1987), mechanisms must exist to make nucleosomes in CDSs accessible to elongating polymerases. The presence of shorter (<130 bp) MPDFs in CDSs of transcribed genes indicates the generation of MNase-sensitive/accessible nucleosomes in a transcription-dependent manner (Figure 1B). Although, elongating polymerase are shown to generate hexosomes and disrupt chromatin structure (Kireeva et al.2002; Ramachandran and Henikoff 2016a), it is likely other factors, such as chromatin remodelers, can further aid in making nucleosomes accessible for elongating polymerases. However, it is not clear which remodelers might help in this process. RSC and SWI/SNF have both histone sliding and histone eviction activities (Boeger et al.2004; Montel et al.2011; Clapier et al.2017) and are shown to be present in CDSs of transcribed genes (Yen et al.2012; Ganguli et al.2014; Spain et al.2014; Rawal et al.2018; Vinayachandran et al.2018). In addition, RSC is shown to promote Pol II elongation, *in vitro*, through acetylated nucleosomes (Carey et al.2006). It has been reported that RSC bound nucleosomes in

NDRs are “fragile,” suggesting that RSC might expose DNA and makes nucleosomes sensitive to MNase digestion (Kubik et al.2015; Brahma and Henikoff 2019). Although there is controversy regarding fragile nucleosomes in NDRs (Chereji et al.2017), it is clear that RSC makes nucleosomes accessible (Clapier et al.2017; Cakiroglu et al.2019). Considering that promoter nucleosomes are the most accessible, we propose that RSC generates accessible “promoter-like” nucleosome in CDSs to promote transcription. This is supported by the data showing that SM-induced genes, which are generally transcribed at very low-levels, show increased presence of shorter MPDFs (<130 bp; Figure 1D) consistent with increased RSC recruitment to their CDSs upon transcription induction (Spain et al.2014; Rawal et al.2018). And likewise, nuclear depletion of TBP, which is needed for PIC assembly and transcription, significantly reduces the presence of accessible nucleosomes (Figure 1E; (Kubik et al.2018)). This suggests that accessible nucleosomes are generated during transcription. Pol II elongation through nucleosomes, *in vitro*, has been shown to displace H2A/H2B dimer, and could contribute to shorter MPDFs, observed *in vivo* (Figure 1) (Izban and Luse 1991; Kireeva et al.2002). In addition, we find that RSC-bound nucleosomes displayed very heterogenous MPDF lengths, which might represent nucleosome remodeling intermediates. Consistent with the idea that high-levels of transcription might require more frequent remodeling, we find a higher proportion of shorter MPDFs at very highly transcribed genes, including at the RPGs (Figure 4).

Our study also suggests that RSC-mediated remodeling in CDSs might also promote transcription. Given the established role for RSC in maintaining NDRs and in positioning the flanking -1 and +1 nucleosomes, it makes sense that cells with diminished RSC function would show transcription defects. The defects in transcription observed in RSC mutants are attributed to reduced TBP binding and TSS-site selection (Kubik et al.2018; Rawal et al.2018; Klein-Brill et al.2019; Kubik et al.2019). Given an intricate relationship between transcription and RSC recruitment to CDSs (Spain et al.2014; Rawal et al.2018), it is extremely difficult to separate effects of RSC and of Pol II on nucleosome structure. In fact both RSC-bound and Pol II-bound nucleosomes are more

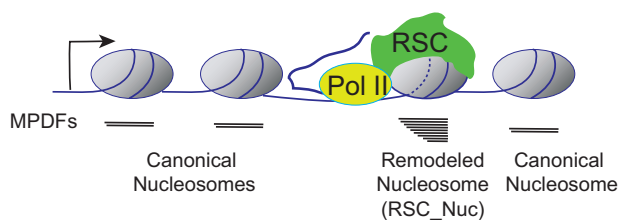


Figure 8 Model. According to this model, RSC targets the nucleosomes immediately downstream of the elongating RNA polymerase II (Pol II). The remodeling status of nucleosome is depicted by the dashed lines (–), and this nucleosome is in close proximity to Pol II. The nucleosome undergoing RSC-mediated remodeling will have DNA more accessible to MNase, yielding a heterogeneous MNase protected DNA fragments (MPDFs) ranging from 80 to 160 bp compared to a sharper MPDF profile for canonical nucleosomes. The recruitment of RSC to the nucleosome could be facilitated by either direct interaction with Pol II (Soutourina et al. 2006), or through phosphorylated C-terminal domain (CTD) of Pol II and transient acetylation by histone acetyltransferases SAGA and NuA4 (Govind et al. 2007; Ginsburg et al. 2009; Spain et al. 2014). Resetting of the nucleosome to a canonical conformation can be achieved by rapid deacetylation by histone deacetylase complexes, such as Rpd3-small and Hos2-Set3C in a manner dependent on histone methylation (Carozza et al. 2005; Kim and Buratowski 2009; Govind et al. 2010).

MNase-accessible compared to canonical nucleosomes in CDSs (Figures 4 and 5). However, the analyses presented in the current study also points to a potential role for RSC in genic nucleosome accessibility. Rapid nuclear depletion of RSC ATPase Sth1 elicited higher Pol II occupancies in CDSs of highly transcribed genes notwithstanding reduced TBP binding (Figure 6). Considering that reduced TBP binding is expected to decrease Pol II occupancies, not increase, (Petrenko et al. 2019) increased Pol II occupancy in genic regions is consistent with reduced elongation rate. One possible explanation for this is that elongating polymerases find it difficult to navigate in absence of RSC-mediated remodeling of nucleosomes in CDSs, which thereby increases their dwell-time leading to increased ChIP efficiency. As noted earlier, comparison of nascent RNA levels and Pol II occupancies in cells deficient for RSC function could provide stronger support to the role for RSC in promoting Pol II elongation. Considering that RSC is present in both promoters (Kubik et al. 2019) and in CDSs (Spain et al. 2014; Rawal et al. 2018) (Figure 4), our study suggests that in addition to RSC regulating PIC assembly and TSS-site selection, RSC may also stimulate transcription by remodeling nucleosomes in CDSs for efficient Pol II elongation. The idea that RSC promotes transcription elongation is supported by *in vitro* experiments showing RSC remodeled nucleosomes promote transcription elongation in an acetylation-dependent manner (Carey et al. 2006).

We note that the profile for nucleosomes (MNase inputs) did not show the fragment heterogeneity that is observed for the RSC-bound nucleosomes, implying that only a small fraction of nucleosomes within a gene are accessible at any given time. We speculate that the nucleosomes immediately downstream of the elongating polymerases might be targeted by RSC and rendered accessible, whereas other nucleosomes will be in a canonical conformation (largely inaccessible; MPDF >130 bp) (Figures 4 and 8). In agreement with this, the Pol II-bound nucleosomes also displayed significant proportions of shorter MPDFs similar to that observed for RSC-bound nucleosomes, suggesting that Pol II either generates or accesses MNase-sensitive nucleosomes in CDSs. We favor a model in which initial disruption of nucleosomes by elongating Pol II facilitate RSC to be recruited in CDSs and remodel nucleosomes to promote transcription elongation and to achieve high rates of transcription. As such RPGs

shows both high RSC occupancies and high-levels of RSC-bound MNase-accessible nucleosomes (Figure 4) and loss of RSC reduces nucleosome accessibility (Figure 7A).

Previous studies, including ours, have provided support for the idea that RSC interacts with elongating Pol II via the Rsc4 subunit or in a manner dependent on Pol II CTD phosphorylation (Soutourina et al. 2006; Spain et al. 2014). Rsc4 has also been shown to recognize acetylated H3K14 *in vitro* (Kasten et al. 2004). It is therefore possible that RSC uses Rsc4, along with other bromodomain-containing subunits, to recognize Pol II-proximal nucleosomes, which are transiently acetylated by the SAGA and NuA4 HAT complexes (Kasten et al. 2004; Govind et al. 2007; Ginsburg et al. 2009). Acetylation of nucleosomes has also been implicated in enhancing remodeling by the RSC complex (Chatterjee et al. 2011; 2015) and has been shown to promote RSC recruitment to transcribed CDSs (Spain et al. 2014). Thus, RSC-bound nucleosomes might resemble promoter nucleosomes in that these nucleosomes will be hyperacetylated and susceptible to MNase digestion. The remodeling by RSC may be limited to nucleosomes immediately downstream of the elongating Pol II (Figure 8), as nucleosomes upstream of the Pol II would be deacetylated by the Hos2-Set1 and Rpd3(S)-Set2 pathways (Carozza et al. 2005; Kim and Buratowski 2009; Govind et al. 2010). These complexes are shown to interact with phosphorylated Pol II and deacetylate CDSs nucleosomes in a manner dependent on histone methylation. The idea that RSC provides transient access to nucleosomal DNA in an acetylation-dependent manner might also provide an explanation as to why cryptic transcription initiation occurs from within CDSs in cells deficient of histone deacetylase or histone methyltransferase function (Carozza et al. 2005).

Acknowledgement

We thank Dr. Alan Hinnebusch, Dr. David Clark, and Dr. Gabriel Zentner for providing useful comments on the manuscript.

Funding

This work was supported by National Institutes of Health grants R01GM095514 and R15GM126449 to CKG, and from Center for Biomedical Sciences, Oakland University.

Declaration of interest

The authors declare no competing interests.

Author contributions

Conceptualization:CKG and EB.Methodology:CKG, JK, and EB.Investigation:CKG, JK, EB, KD, CR.Writing:CKG, EB and KD.Supervision:CKG.Administration:CKG.Funding Acquisition:CKG.

References

- BadisG, ChanET, van BakelH, Pena-CastilloL, TilloD, et al. 2008. A library of yeast transcription factor motifs reveals a widespread function for Rsc3 in targeting nucleosome exclusion at promoters. *Mol Cell.* 32:878–887.
- BoegerH, GriesenbeckJ, Strattan JS, KornbergRD. 2004. Removal of promoter nucleosomes by disassembly rather than sliding *in vivo*. *Mol Cell.* 14:667–673.

- BondarenkoVA, SteeleLM, UjvariA, GaykalovaDA, KulaevaOI, et al. 2006. Nucleosomes can form a polar barrier to transcript elongation by RNA polymerase II. *Mol Cell*. 24:469–479.
- BrahmaS, HenikoffS. 2019. RSC-associated subnucleosomes define MNase-sensitive promoters in yeast. *Mol Cell*. 73:238–249. e233.
- CairnsBR, LorchY, LiY, ZhangM, LacomisL, et al. 1996. RSC, an essential, abundant chromatin-remodeling complex. *Cell*. 87:1249–1260.
- CakirogluA, ClapierCR, EhrensbergerAH, DarboE, CairnsBR, et al. 2019. Genome-wide reconstitution of chromatin transactions reveals that RSC preferentially disrupts H2AZ-containing nucleosomes. *Genome Res*. 29:988–998.
- CareyM, Li B, WorkmanJL. 2006. RSC exploits histone acetylation to abrogate the nucleosomal block to RNA polymerase II elongation. *Mol Cell*. 24:481–487.
- CarrozzaMJ, LiB, FlorensL, SuganumaT, SwansonSK, et al. 2005. Histone H3 methylation by Set2 directs deacetylation of coding regions by Rpd3S to suppress spurious intragenic transcription. *Cell*. 123:581–592.
- ChatterjeeN, NorthJA, DechassaML, ManoharM, PrasadR, et al. 2015. Histone acetylation near the nucleosome dyad axis enhances nucleosome disassembly by RSC and SWI/SNF. *Mol Cell Biol*. 35:4083–4092.
- ChatterjeeN, SinhaD, Lemma-DechassaM, TanS, Shogren-KnaakMA, et al. 2011. Histone H3 tail acetylation modulates ATP-dependent remodeling through multiple mechanisms. *Nucleic Acids Res*. 39:8378–8391.
- CherejiRV, Ocampo J, ClarkDJ. 2017. MNase-sensitive complexes in yeast: nucleosomes and non-histone barriers. *Mol Cell*. 65:565–577 e563.
- CherejiRV, RamachandranS, Bryson TD, HenikoffS. 2018. Precise genome-wide mapping of single nucleosomes and linkers in vivo. *Genome Biol*. 19:19.
- ChurchmanLS, WeissmanJS. 2011. Nascent transcript sequencing visualizes transcription at nucleotide resolution. *Nature*. 469:368–373.
- ClapierCR, CairnsBR. 2009. The biology of chromatin remodeling complexes. *Annu Rev Biochem*. 78:273–304.
- ClapierCR, IwasaJ, Cairns BR, PetersonCL. 2017. Mechanisms of action and regulation of ATP-dependent chromatin-remodelling complexes. *Nat Rev Mol Cell Biol*. 18:407–422.
- ClapierCR, KastenMM, ParnellTJ, ViswanathanR, SzerlongH, et al. 2016. Regulation of DNA translocation efficiency within the chromatin remodeler RSC/Stb1 potentiates nucleosome sliding and ejection. *Mol Cell*. 62:453–461.
- DionMF, KaplanT, KimM, BuratowskiS, FriedmanN, et al. 2007. Dynamics of Replication-Independent Histone Turnover in Budding Yeast. *Science*. 315:1405–1408.
- FarnungL, Vos SM, CramerP. 2018. Structure of transcribing RNA polymerase II-nucleosome complex. *Nat Commun*. 9:5432.
- GanguliD, CherejiRV, IbenJR, Cole HA, ClarkDJ. 2014. RSC-dependent constructive and destructive interference between opposing arrays of phased nucleosomes in yeast. *Genome Res*. 24:1637–1649.
- GinsburgDS, Govind CK, HinnebuschAG. 2009. NuA4 lysine acetyltransferase Esa1 is targeted to coding regions and stimulates transcription elongation with Gcn5. *MCB*. 29:6473–6487.
- GovindCK, Ginsburg D, HinnebuschAG. 2012. Measuring dynamic changes in histone modifications and nucleosome density during activated transcription in budding yeast. *Methods Mol Biol*. 833:15–27.
- GovindCK, QiuH, GinsburgDS, RuanC, HofmeyerK, et al. 2010. Phosphorylated Pol II CTD recruits multiple HDACs, including Rpd3C(S), for methylation-dependent deacetylation of ORF nucleosomes. *Mol Cell*. 39:234–246.
- GovindCK, YoonS, QiuH, Govind S, HinnebuschAG. 2005. Simultaneous recruitment of coactivators by Gcn4p stimulates multiple steps of transcription in vivo. *MCB*. 25:5626–5638.
- GovindCK, ZhangF, QiuH, Hofmeyer K, HinnebuschAG. 2007. Gcn5 promotes acetylation, eviction, and methylation of nucleosomes in transcribed coding regions. *Mol Cell*. 25:31–42.
- HartleyPD, MadhaniHD. 2009. Mechanisms that Specify Promoter Nucleosome Location and Identity. *Cell*. 137:445–458.
- HarukiH, Nishikawa J, LaemmliUK. 2008. The anchor-away technique: rapid, conditional establishment of yeast mutant phenotypes. *Mol Cell*. 31:925–932.
- HenikoffJG, BelskyJA, KrassovskyK, MacAlpine DM, HenikoffS. 2011. Epigenome characterization at single base-pair resolution. *Proc Natl Acad Sci*. 108:18318–18323.
- IzbanMG, LuseDS. 1991. Transcription on nucleosomal templates by RNA polymerase II in vitro: inhibition of elongation with enhancement of sequence-specific pausing. *Genes Dev*. 5:683–696.
- KastenM, SzerlongH, Erdjument-BromageH, TempstP, WernerM, et al. 2004. Tandem bromodomains in the chromatin remodeler RSC recognize acetylated histone H3 Lys14. *Embo J*. 23:1348–1359.
- KimT, BuratowskiS. 2009. Dimethylation of H3K4 by Set1 recruits the Set3 histone deacetylase complex to 5' transcribed regions. *Cell*. 137:259–272.
- KireevaML, WalterW, TchernajenkoV, BondarenkoV, KashlevM, et al. 2002. Nucleosome remodeling induced by RNA polymerase II: loss of the H2A/H2B dimer during transcription. *Mol Cell*. 9:541–552.
- Klein-Brilla, Joseph-StraussD, Appleboim A, FriedmanN. 2019. Dynamics of chromatin and transcription during transient depletion of the rsc chromatin remodeling complex. *Cell Rep*. 26:279–292.e275.
- KoerberRT, RheeHS, Jiang C, PughBF. 2009. Interaction of transcriptional regulators with specific nucleosomes across the *Saccharomyces* genome. *Mol Cell*. 35:889–902.
- KrietensteinN, WalM, WatanabeS, ParkB, PetersonCL, et al. 2016. Genomic Nucleosome Organization Reconstituted with Pure Proteins. *Cell*. 167:709–721 e712.
- KubikS, BruzzoneMJ, ChallalD, DreosR, MattarocciS, et al. 2019. Opposing chromatin remodelers control transcription initiation frequency and start site selection. *Nat Struct Mol Biol*. 26:744–754.
- KubikS, BruzzoneMJ, JacquetP, FalconeJL, RougemontJ, et al. 2015. Nucleosome stability distinguishes two different promoter types at all protein-coding genes in yeast. *Mol Cell*. 60:422–434.
- KubikS, Bruzzone MJ, ShoreD. 2017. Establishing nucleosome architecture and stability at promoters: roles of pioneer transcription factors and the RSC chromatin remodeler. *Bioessays*. 1600237.39.
- KubikS, O'DuibhirE, de JongeWJ, MattarocciS, AlbertB, et al. 2018. Sequence-directed action of RSC remodeler and general regulatory factors modulates +1 nucleosome position to facilitate transcription. *Mol Cell*. 71:89–102 e105.
- KujiraiT, EharaH, FujinoY, ShirouzuM, SekineS-I, et al. 2018. Structural basis of the nucleosome transition during RNA polymerase II passage. *Science*. 362:595–598.
- KulaevaOI, Gaykalova DA, StuditskyVM. 2007. Transcription through chromatin by RNA polymerase II: histone displacement and exchange. *Mutat Res*. 618:116–129.

- KulaevaOI, HsiehFK, ChangHW, Luse DS, StuditskyVM. 2013. Mechanism of transcription through a nucleosome by RNA polymerase II. *Biochim Biophys Acta*. 1829:76–83.
- LorchY, LaPointe JW, KornbergRD. 1987. Nucleosomes inhibit the initiation of transcription but allow chain elongation with the displacement of histones. *Cell*. 49:203–210.
- MontelF, CastelnovoM, MenoniH, AngelovD, DimitrovS, et al. 2011. RSC remodeling of oligo-nucleosomes: an atomic force microscopy study. *Nucleic Acids Res*. 39:2571–2579.
- MusladinS, KrietensteinN, Korber P, BarbaricS. 2014. The RSC chromatin remodeling complex has a crucial role in the complete remodeler set for yeast PHO5 promoter opening. *Nucleic Acids Res*. 42:4270–4282.
- NatarajanK, MeyerMR, JacksonBM, SladeD, RobertsC, et al. 2001. Transcriptional profiling shows that Gcn4p is a master regulator of gene expression during amino acid starvation in yeast. *Mol Cell Biol*. 21:4347–4368.
- NishimuraK, FukagawaT, TakisawaH, Kakimoto T, KanemakiM. 2009. An auxin-based degron system for the rapid depletion of proteins in nonplant cells. *Nat Methods*. 6:917–922.
- OcampoJ, CherejiRV, Eriksson PR, ClarkDJ. 2019. Contrasting roles of the RSC and ISW1/CHD1 chromatin remodelers in RNA polymerase II elongation and termination. *Genome Res*. 29:407–417.
- PetrenkoN, JinY, DongL, Wong KH, StruhlK. 2019. Requirements for RNA polymerase II preinitiation complex formation in vivo. *Elife*. 8.
- RamachandranS, Ahmad K, HenikoffS. 2017. Transcription and Remodeling Produce Asymmetrically Unwrapped Nucleosomal Intermediates. *Mol Cell*. 68:1038–1053 e1034.
- RamachandranS, HenikoffS. 2016a. Nucleosome dynamics during chromatin remodeling in vivo. *Nucleus*. 7:20–26.
- RamachandranS, HenikoffS. 2016b. Transcriptional regulators compete with nucleosomes post-replication. *Cell*. 165:580–592.
- RamachandranS, Zentner GE, HenikoffS. 2015. Asymmetric nucleosomes flank promoters in the budding yeast genome. *Genome Res*. 25:381–390.
- RawalY, CherejiRV, QiuH, AnanthakrishnanS, GovindCK, et al. 2018. SWI/SNF and RSC cooperate to reposition and evict promoter nucleosomes at highly expressed genes in yeast. *Genes Dev*. 32:695–710.
- ShuklaMS, SyedSH, MontelF, Faivre-MoskalenkoC, BednarJ, et al. 2010. Remosomes: RSC generated non-mobilized particles with approximately 180 bp DNA loosely associated with the histone octamer. *Proc Natl Acad Sci USA*. 107:1936–1941.
- SoutourinaJ, Bordas-Le FlochV, GendrelG, FloresA, DucrotC, et al. 2006. Rsc4 connects the chromatin remodeler RSC to RNA polymerases. *MCB*. 26:4920–4933.
- SpainMM, AnsariSA, PathakR, PalumboMJ, MorseRH, et al. 2014. The RSC complex localizes to coding sequences to regulate Pol II and histone occupancy. *Mol Cell*. 56:653–666.
- SpainMM, GovindCK. 2011. A role for phosphorylated Pol II CTD in modulating transcription coupled histone dynamics. *Transcription*. 2:78–81.
- UjvariA, HsiehFK, LuseSW, Studitsky VM, LuseDS. 2008. Histone N-terminal tails interfere with nucleosome traversal by RNA polymerase II. *J Biol Chem*. 283:32236–32243.
- VinayachandranV, RejaR, RossiMJ, ParkB, RieberL, et al. 2018. Widespread and precise reprogramming of yeast protein-genome interactions in response to heat shock. *Genome Res*. 28:357–366.
- WeberCM, Ramachandran S, HenikoffS. 2014. Nucleosomes are context-specific, H2A.Z-modulated barriers to RNA polymerase. *Mol Cell*. 53:819–830.
- XuZ, WeiW, GagneurJ, PerocchiF, Clauder-MünsterS, et al. 2009. Bidirectional promoters generate pervasive transcription in yeast. *Nature*. 457:1033–1037.
- YenK, VinayachandranV, BattaK, Koerber RT, PughBF. 2012. Genome-wide nucleosome specificity and directionality of chromatin remodelers. *Cell*. 149:1461–1473.

Communicating editor: C. D. Kaplan